Kay, W. B., "Density of Hydrocarbon Gases and Vapors at High Temperature and Pressure," *Ind. Eng. Chem.*, **28**, 1014 (1936).
Klosek, J., and C. McKinley, "Densities of Liquified Natural Gas and of Low Molecular Weight Hydrocarbons," *Proc. First Int. Conf. on LNG*, Session 5, Paper 22, Chicago, Ill. (1968).
Kudchadker, A. P., G. H. Alani, and B. J. Zwolinski, "The Critical Constants of Organic Substances," *Chem. Rev.*, **68**, 659 (1968).
Lee, B. I., and M. G. Kesler, "A Generalized Thermodynamic Correlation Based on Three-Parameter Corresponding States," *AIChE J.*, **21**, 510 (1975).
Mathews, J. F., "The Critical Constants of Inorganic Substances," *Chem. Rev.*, **72**, 71 (1972).
McCarty, R. D., "A Modified Benedict-Webb-Rubin Equation of State for Methane Using Recent Experimental Data," *Cryogenics*, **14**, 276 (1974).
Mollerup, J., and J. S. Rowlinson, "The Prediction of Densities of Liquified Natural Gas and of Lower Molecular Weight Hydrocarbons," *Chem. Eng. Sci.*, **29**, 1373 (1974).
Passut, C. A., and R. D. Danner, "Acentric Factor. A Valuable Correlating Parameter for the Properties of Hydrocarbons," *Ind. Eng. Chem. Process Design Develop.*, **12**, 365 (1973).
Prausnitz, J. M., and P. L. Chueh, *Computer Calculations for High-Pressure Vapor-Liquid Equilibria*, Prentice-Hall, Englewood Cliffs, N.J. (1968).
Rackett, H. G., "Equation of State for Saturated Liquids," *J. Chem. Eng. Data*, **15**, 514 (1970).
Soave, G., "Equilibrium Constants from a Modified Redlich-Kwong Equation of State," *Chem. Eng. Sci.*, **27**, 1197 (1972).
Spencer, C. F., and S. B. Adler, "A Critical Review of Equations for Predicting Saturated Liquid Density," *J. Chem. Eng. Data*, **23**, No. 1, 82 (1978).
Spencer, C. F., and R. P. Danner, "Improved Equation for Prediction of Saturated Liquid Density," *ibid.*, **17**, 236 (1972).
———, "Prediction of Bubble-Point Density of Mixtures," *ibid.*, **18**, No. 2, 230 (1973).
Yen, L. C., and S. S. Woods, "A Generalized Equation for Computer Calculation of Liquid Densities," *AIChE J.*, **12**, 95 (1966).
Yu, P., and B. C.-Y. Lu, "Prediction of Saturated Liquid Densities of LNG Mixtures," *Ind. Eng. Chem. Process Design Develop.*, **15**, 221 (1976).

Supplementary material has been deposited as Document No. 03437 with the National Auxiliary Publications Service (NAPS), c/o Microfiche Publications, 214-13 Jamaica Ave., Queens Village, N.Y. 11428.
Manuscript received September 6, 1978; revision received March 19, and accepted March 29, 1979.

Theoretical Prediction of Effective Heat Transfer Parameters in Packed Beds

ANTHONY G. DIXON
and
DAVID L. CRESSWELL
Systems Engineering Group
E.T.H.-Zentrum
CH-8092 Zurich, Switzerland

A theory for predicting the effective axial and radial thermal conductivities and the apparent wall heat transfer coefficient for fluid flow through packed beds is derived from a two-phase continuum model containing the essential underlying and independently measurable heat transfer processes. The theory is shown to explain much of the confused literature and pinpoints the remaining major areas of uncertainty, further investigation of which is needed before secure prediction is possible.

SCOPE

Knowledge of the effective thermal conductivity and wall heat transfer coefficient for fluid flow through packed tubular beds forms an important aspect in the design of catalytic reactors.

In studying heat transfer in packed beds, we attempt to answer the following question: Given the mass velocity of the fluid, the mean bed voidage, the tube diameter, the particle size, shape and conductivity, and the essential physical properties of the fluid such as the viscosity, specific heat, and molecular conductivity, what values do the effective axial and radial conductivity of the bed and the wall heat transfer coefficient take? This question has dogged researchers for the past 25 yr, and, despite the vast literature, no satisfactory answer has been found. Nor will it be answered, we believe, by producing yet more empirical correlations.

The main objective of this paper and contribution to the profession, we hope, is to direct attention towards a theoretical, rather than empirical, approach. By theoretical approach, we imply the development of a model relating effective heat transfer parameters to the essential underlying and independently measurable heat transfer processes. Thus, no empirical or adjustable constants are involved. We have accounted for seven such basic heat transfer steps which we have felt necessary to review in the middle part of our paper.

The predictions of the theory are compared with reliable literature data for qualitative trends in parameter relations as much as for absolute accuracy. We feel that a thorough testing of our theory must await further experimental work on several of the basic heat transfer steps.

Correspondence concerning this paper should be addressed to David L. Cresswell. Anthony G. Dixon is at the Mathematics Research Center, University of Wisconsin, Madison, Wisconsin 53706.

CONCLUSIONS AND SIGNIFICANCE

The significance of this work is, we believe, that for the first time we have a theoretical model which provides a systematic framework for building up estimates of effective thermal conductivities and wall heat transfer coefficient from clearly identifiable basic heat transfer steps.

We have tried to test this model as far as is possible against reliable literature data, but a thorough examination must await further research into several of the basic heat transfer steps.

In discussing our conclusions it is perhaps best to deal with each parameter in turn.

1. Wall Heat Transfer Coefficient ($h_{w,\text{eff}}$). Our theory shows that if the wall heat transfer coefficient is correlated in terms of a Biot number rather than a Nusselt number, as has been the normal practice, a unique relationship with Reynolds number should occur, independent of particle size or conductivity. In particular, it was found that the theoretically derived relation

$$Bi\left(\frac{d_p}{R}\right) = 3.0\,Re^{-0.25} \quad (Re > 40)$$

predicted adequately wall heat transfer coefficients over a wide range of conditions.

On the other hand, the *Nu* vs. *Re* relation is nonunique but depends on several factors, such as the tube/particle diameter ratio, the pellet conductivity, the fluid/solid heat transfer coefficient, the radial fluid conductivity, and the solid/wall heat transfer coefficient.

The apparently large scatter of *Nu* vs. *Re* correlations, which has been a source of much investigation, is no more than a failure to recognize these additional factors.

2. The Effective Radial Conductivity ($k_{r,\text{eff}}$). This is the most accurately predicted heat transfer parameter. A somewhat simplified case of the general relationship that we have tested against experimental data may be written as

$$k_{r,\text{eff}} = k_{rf} + k_{rs}\left[\frac{1 + \dfrac{8\,k_{rf}}{h_{wf}d_t}}{1 + \dfrac{\dfrac{16}{3}k_{rs}\left(\dfrac{1}{h_{fs}d_p} + \dfrac{0.1}{k_p}\right)}{(1-\epsilon)\left(\dfrac{d_t}{d_p}\right)^2}}\right]$$

Thus, the effective conductivity depends not only on the conductivities of the two phases, as has been thought previously, but also on additional parameters, such as the fluid/wall heat transfer coefficient, the fluid/solid heat transfer coefficient, the particle diameter, and the tube/particle diameter ratio.

Only in the limit $d_t/d_p \to \infty$ is it strictly permissible to treat the effective conductivity as the sum of the conductivities of the two phases existing in parallel.

The effective radial conductivity can be predicted to within a few percent over a wide range of *Re* and d_t/d_p ratio. This compares with empirical correlations which are accurate to within 25% for nonmetallic packings and 50% or worse for metallic packings.

3. The Effective Axial Conductivity ($k_{a,\text{eff}}$). This is perhaps the least accurately predicted heat transfer parameter. The analogous relationship for the effective axial conductivity that we have used in our comparison with literature data is given by

$$k_{a,\text{eff}} = k_{af} + \left[\frac{k_{as}}{1 + \dfrac{\dfrac{16}{3}k_{as}\left(\dfrac{1}{h_{fs}d_p} + \dfrac{0.1}{k_p}\right)}{(1-\epsilon)\left(\dfrac{d_t}{d_p}\right)^2}}\right]^2$$

The effective axial conductivity depends not only on the axial conductivities of the two phases but also on the fluid/solid heat transfer coefficient, the particle diameter, and the tube/particle diameter ratio.

Only in the limit $d_t/d_p \to \infty$ is it strictly permissible to treat the effective conductivity as the sum of the conductivities of the two phases existing in parallel.

At present, it is not possible to test the equation over a wide range of conditions, since two of the basic steps in the theory are far from resolved. These concern axial gas mixing studies at moderate *Re* for systems having low d_t/d_p ratio (from which k_{af} can be determined) and fluid/solid heat transfer studies conducted at low *Re*, for which there is considerable disagreement in the literature.

An important conclusion which was reached in the course of testing the theory is that much of the literature data on heat transfer is extremely unreliable.

We implore future experimenters to address themselves to the following questions:

1. Is the type of experiment conducted satisfactory for the reliable determination of effective heat transfer parameters?
2. Is the model used in the analysis of the data adequate or have significant terms been omitted?
3. Is the method of analysis statistically sound in the face of experimental errors?

We hope that this work will stimulate further research into heat transfer in packed beds, particularly into studies of some of the basic heat transfer steps which are still poorly understood. In particular, there is a need for work in the following areas:

1. Axial dispersion studies at small d_t/d_p ratio ($d_t/d_p \sim$ 3-12) over an extended range of *Re*.
2. Solid/fluid heat or mass transfer studies at low *Re*.
3. Wall/fluid mass transfer studies at low *Re* (< 100) for gases (from which wall/fluid heat transfer coefficients can be estimated).
4. Wall/solid heat transfer.

In spite of 25 yr of active research, today's chemical engineer has at his disposal but a handful of empirical correlations for predicting effective heat transfer parameters in packed beds. The majority of these correlations show different functional dependencies, and all of them are specific to the given system and range of operating conditions over which they were fitted to the data. While these researches have often given valuable insight into the nature of the individual heat transfer processes involved, the integration of these steps into a reliable model for

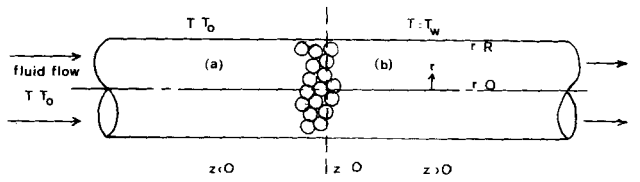

Fig. 1. Schematic representation of packed bed.

predicting effective heat transfer parameters has so far remained elusive, and it forms one of the principal objectives of current heat transfer research.

As a starting point for a predictive method, we consider a diffusional model of the heat transfer processes which allows for different temperature profiles in the solid and fluid phases similar to that described by Olbrich (1970) but generalized to include axial conduction in both the fluid and solid. This model contains many, if not all, of the basic heat transfer parameters which are believed to be significant and which can be determined experimentally. A semianalytical solution of this model can be obtained by a combined collocation-perturbation technique. This solution is then compared with a similar one-point collocation solution of the simpler pseudohomogeneous model containing effective conductivities and apparent wall heat transfer coefficient. Relations between the parameters of the two models are found by exactly matching the fluid-phase temperature distribution in the two-phase model with the one-phase model solution. In deriving these relations, it is unnecessary to assume that solid and fluid temperatures are equal or that their second derivatives in the axial direction are equal (Vortmeyer and Schaefer, 1974), both assumptions severely restricting the validity of the relations. The ability of this approach to explain both qualitative and quantitative aspects of published data is examined.

THEORETICAL BACKGROUND

We shall consider a packed tubular heat exchanger of the form used in recent experimental studies (Gunn and Khalid, 1975; Dixon et al., 1978*a*). The bed consists of an unheated long calming section (a) and a heated test section (b), the walls of which are insulated from each other at the plane $z = 0$, as in Figure 1. Both sections are packed with similar solid particles to provide a continuous length of packing. It is assumed that the fluid entering the section (a) and the wall of section (a) are at the same temperature T_o, the wall of the heated section being at T_w.

In setting up the model, it will be assumed that the temperature variations within particles may be smoothed so that only large scale changes in solid temperature in the axial and radial directions need be considered. A similar approach is adopted for the fluid. If we assume constancy of physical properties and the fluid to be in axially dispersed plug flow, the following differential heat balances may be set up:

Fluid phase

$$k_{rf}\left(\frac{\partial^2 T}{\partial r^2}+\frac{1}{r}\frac{\partial T}{\partial r}\right)+k_{af}\frac{\partial^2 T}{\partial z^2} - ah(T-t)=Gc_p\frac{\partial T}{\partial z} \quad (1)$$

Solid phase

$$k_{rs}\left(\frac{\partial^2 t}{\partial r^2}+\frac{1}{r}\frac{\partial t}{\partial r}\right)+k_{as}\frac{\partial^2 t}{\partial z^2}+ah(T-t)=0 \quad (2)$$

with boundary conditions

$$\frac{\partial T}{\partial r}=\frac{\partial t}{\partial r}=0 \qquad \text{at } r=0 \quad (3)$$

$$-k_{rf}\frac{\partial T}{\partial r}=h_{wf}(T-T_w) \qquad \text{at } r=R,\ z>0 \quad (4)$$

$$-k_{rf}\frac{\partial T}{\partial r}=h_{wf}(T-T_o) \qquad \text{at } r=R,\ z<0 \quad (5)$$

$$-k_{rs}\frac{\partial t}{\partial r}=h_{ws}(t-T_w) \qquad \text{at } r=R,\ z>0 \quad (6)$$

$$-k_{rs}\frac{\partial t}{\partial r}=h_{ws}(t-T_o) \qquad \text{at } r=R,\ z<0 \quad (7)$$

$$t, T \to T_o \quad \text{as} \quad z \to -\infty \quad (8)$$

$$t, T \to T_w \quad \text{as} \quad z \to +\infty \quad (9)$$

$$T(0^+)=T(0^-);\quad t(0^+)=t(0^-) \quad (10)$$

$$\frac{\partial T(0^+)}{\partial z}=\frac{\partial T(0^-)}{\partial z};\quad \frac{\partial t(0^+)}{\partial z}=\frac{\partial t(0^-)}{\partial z} \quad (11)$$

A discussion of the physical significance of the parameters and their estimation is given later.

ANALYSIS OF THE TWO-PHASE MODEL

Olbrich (1970) obtained an exact analytical solution of the two-phase model by neglecting axial conduction terms in both phases. Unfortunately, inclusion of these terms alters the nature of the problem and greatly complicates the mathematical solution. Since matching of models in this context usually means equating the first terms of respective infinite series solutions which is, in itself, an approximate procedure and which also leads to implicit relations between parameters, we prefer at the outset to derive approximate solutions of the models which then lead to explicit parameter relations. As a basis we employ a collocation-perturbation technique, details of which are given in the Appendix. It is shown there that the dimensionless temperature distribution in the fluid phase is given approximately by

$$T^*(x,y)=\begin{cases}1+\left\{\dfrac{Bi_f(y^2-1)-2}{Bi_f+4}\right\}\left(\dfrac{1+\beta}{\beta}\right) \\ \qquad (x>0) \\ \qquad\qquad \exp\left\{\dfrac{\hat{Pe}_{AF}(1-\beta)x}{2}\right\} \\ \left\{\dfrac{Bi_f(y^2-1)-2}{Bi_f+4}\right\}\left(\dfrac{1-\beta}{\beta}\right) \\ \qquad (x<0) \\ \qquad\qquad \exp\left\{\dfrac{\hat{Pe}_{AF}(1+\beta)x}{2}\right\}\end{cases} \quad (12)$$

The solid-phase temperature distribution $t^*(x, y)$ is not considered in the model matching procedure and, therefore, is not given here. However, solid-phase temperature profiles are considered in the Appendix.

ANALYSIS OF THE PSEUDOHOMOGENEOUS MODEL

Temperature measurements in a packed bed are invariably analyzed by a pseudohomogeneous model which makes no distinction between the fluid and solid temperatures. A differential heat balance for this model leads to

the equation

$$k_{r,\text{eff}}\left(\frac{\partial^2 T_b}{\partial r^2}+\frac{1}{r}\frac{\partial T_b}{\partial r}\right)+k_{a,\text{eff}}\frac{\partial^2 T_b}{\partial z^2}=Gc_p\frac{\partial T_b}{\partial z} \quad (13)$$

with boundary conditions

$$\frac{\partial T_b}{\partial r}=0 \qquad \text{at} \quad r=0 \quad (14)$$

$$-k_{r,\text{eff}}\frac{\partial T_b}{\partial r}=h_{w,\text{eff}}\,(T_b-T_w) \quad \text{at} \quad r=R, \quad z>0 \quad (15)$$

$$-k_{r,\text{eff}}\frac{\partial T_b}{\partial r}=h_{w,\text{eff}}\,(T_b-T_o) \quad \text{at} \quad r=R, \quad z<0 \quad (16)$$

$$T_b\to T_o \quad \text{as} \quad z\to-\infty \quad (17)$$

$$T_b\to T_w \quad \text{as} \quad z\to+\infty \quad (18)$$

$$T_b(0^+)=T_b(0^-) \quad (19)$$

$$\frac{\partial T_b(0^+)}{\partial z}=\frac{\partial T_b(0^-)}{\partial z} \quad (20)$$

where $k_{r,\text{eff}}$ and $k_{a,\text{eff}}$ are effective radial and axial bed conductivities, and $h_{w,\text{eff}}$ is the apparent wall heat transfer coefficient.

This model has been shown to provide a statistically adequate description of the temperature distribution in a packed bed (Dixon et al., 1978*b*). A one-point collocation solution of this model gives the dimensionless temperature distribution

$$\theta(x,y)=\begin{cases}1+\left\{\dfrac{Bi(y^2-1)-2}{Bi+4}\right\}\left(\dfrac{1+\beta'}{\beta'}\right) \\ \qquad (x>0) \\ \qquad\qquad \exp\left\{\dfrac{Pe'_A(1-\beta')x}{2}\right\} \\ \left\{\dfrac{Bi(y^2-1)-2}{Bi+4}\right\}\left(\dfrac{1-\beta'}{\beta'}\right) \\ \qquad (x<0) \\ \qquad\qquad \exp\left\{\dfrac{Pe'_A(1+\beta')x}{2}\right\}\end{cases} \quad (21)$$

RELATIONSHIPS BETWEEN MODEL PARAMETERS

The criterion for matching the two models to give relationships between the two sets of parameters is best evaluated by considering the usual experimental procedures for measuring temperatures in a packed bed. These procedures fall into two categories:

1. The radial temperature profile in the fluid leaving the heated bed is measured by an array of thermocouples suspended above the bed (Calderbank and Pogorsky, 1957; DeWasch and Froment, 1972; Dixon et al., 1978*a*).
2. The temperature profile along the central axis ($r=0$) is measured together with the entrance and exit mixing cup temperatures by inserting thermocouples through the wall of the tube at different axial positions (Yagi and Wakao, 1959; Agnew and Potter, 1970).

In the first procedure, it is the fluid-phase temperature profile which is measured, and it is appropriate, therefore, to match the solution of the pseudohomogeneous model with that of the fluid phase in the two-phase model. In the second procedure, it is much less obvious just which temperature is being measured, and it is more appropriate to match the solution of the pseudohomogeneous model with some averaged temperature obtained from the two-phase model, although it is not clear how the averaging should be carried out.

In our experience, the former procedure gives more reliable temperature measurements, permits more data to be gathered, and is more flexible when axial conduction effects must be considered. Since it has also been more widely used than the second procedure, we shall prefer to employ it here.

By inspection of Equations (12) and (21), we may match the model solutions exactly at all points (x, y) by the following dimensionless parameter relations:

$$Bi=Bi_f \quad (22)$$

$$\frac{1}{Pe_A}=\frac{1}{Pe_{AF}}+\frac{(k_{as}/k_g)}{Re\,Pr\left\{1+\dfrac{1}{N_S}\left(\dfrac{8Bi_S}{Bi_S+4}\right)\right\}^2} \quad (23)$$

$$\frac{1}{Pe_R}=\frac{1}{Pe_{RF}}+\frac{(k_{rs}/k_g)}{Re\,Pr}\times\frac{\{(Bi_f+4)/(Bi_f)\}}{\{(8/N_S)+(Bi_s+4)/Bi_s\}} \quad (24)$$

These equations form the most comprehensive relationships so far derived for predicting Bi, Pe_A, and Pe_R and indicate the complexity of the synthesis of underlying heat transfer processes. The terms on the right-hand side of Equations (22) to (24) can be estimated from existing correlations. Thus, no adjustable parameters are involved.

RELEVANT HEAT TRANSFER CORRELATIONS

A brief review of some of the available heat transfer correlations for estimating the dimensionless groups in Equations (22) to (24) is necessary before proceeding with a discussion of the parameter relations.

Effective Radial and Axial Solid Conductivities (k_{rs}, k_{as})

The works of Littmann and Sliva (1970), Kunii and Smith (1961), and Willhite et al. (1962) show that k_{rs}, k_{as} can be treated as stagnant conductivities, independent of fluid flow and, in particular, $k_{as}=k_{rs}$. Zehner and Schlünder (1970) present a correlation for stagnant bed conductivities which gives, for k_{rs}/k_g

$$\frac{k_{rs}}{k_g}=\sqrt{(1-\epsilon)}\times\left(\frac{k^0_{es}}{k_g}\right) \quad (25)$$

where

$$\frac{k^0_{es}}{k_g}=\frac{2}{\left(1-\dfrac{k_g B}{k_p}\right)}\left[\frac{\left(1-\dfrac{k_g}{k_p}\right)B}{\left(1-\dfrac{k_g B}{k_p}\right)^2}\ln\left(\frac{k_p}{B\,k_g}\right)-\frac{B+1}{2}-\frac{B-1}{\left(1-\dfrac{k_g B}{k_p}\right)}\right]$$

with

$$B=C\left(\frac{1-\epsilon}{\epsilon}\right)^{10/9}$$

and

$C=1.25$ for spheres

$=1.4$ crushed particles

$= 2.5$ cylinders/Raschig rings

The Fluid-Phase Radial Peclet Number (Pe_{RF})

This group can be estimated from radial mixing experiments (Fahien and Smith, 1955; Roemer et al., 1962; Gunn and Pryce, 1969). The latter authors suggest an equation for interpolating between molecular and turbulent conduction limits of the form

$$\frac{1}{Pe_{RF}} = \frac{1}{Pe_{RF}(\infty)} + \frac{2/3\epsilon}{Re\,Pr} \tag{26}$$

This equation does not account for the rather weak maximum in the observed Pe_{RF} vs. Re relationship. There is some disagreement as to the value of the turbulent conduction limit $Pe_{RF}(\infty)$. Gunn finds a constant value $Pe_{RF}(\infty) = 11$, independent of the tube/particle diameter ratio (d_t/d_p). However, Fahien and Smith, Roemer et al., and more recently Olbrich and Potter (1972) claim $Pe_{RF}(\infty)$ to be correlated with d_t/d_p, according to

$$Pe_{RF}(\infty) = A\,\{1 + 19.4\,(d_p/d_t)^2\} \tag{27}$$

where A lies between 7 and 10.

An examination of the data of Fahien and Smith reveals that $Pe_{RF}(\infty)$ tends to fluctuate with Re within the range 8 to 12. These fluctuations are such as to render Equation (27) of doubtful validity. At present, the best we can do is take an average value

$$Pe_{RF}(\infty) = 10$$

The Fluid-Phase Axial Peclet Number (Pe_{AF})

Virtually the entire literature on axial gas mixing has been devoted to large diameter beds in which wall effects can be neglected. This case seems to be adequately covered by the data of Edwards and Richardson (1968), which is correlated by

$$\frac{1}{Pe_{AF}} = \frac{0.73\epsilon}{Re\,Pr} + \frac{0.5}{\left(1 + \frac{9.7\epsilon}{Re\,Pr}\right)} \tag{28}$$

an equation whose functional form has been confirmed theoretically by Bischoff (1969).

Unfortunately, Equation (28) appears to seriously overestimate Pe_{AF} for small diameter columns, as indicated by Hsiang and Haynes (1977). There are, as yet, no correlations available for this important case, and considerably more work is needed in this area.

It is interesting to note that the constants in Equations (26) and (28), premultiplying the term $\epsilon/RePr$, are found experimentally to be roughly 0.7, rather than unity, as might be expected. In other words, only 70% of the fluid in the bed is effective for axial and radial mixing, the other 30% being associated with the solid phase, presumably making up the relatively stagnant fluid fillets surrounding the contact points between adjacent pellets. This result is in broad agreement with Zehner and Schlünder's work (1970) on stagnant bed conductivities, which assigned a fraction of $1 - \sqrt{1-\epsilon}$ of the bed volume to the fluid phase, rather than ϵ. Thus, for $\epsilon = 0.4$, only 56% of the fluid in the bed is contributing to heat transfer directly through the fluid phase.

The Fluid/Solid Heat Transfer Coefficient (h)

In smoothing the solid temperature variations, we may regard $t(z, r)$ in Equation (2) as representing the mean temperature of a solid particle at the point (z, r). Consequently, the interphase heat transfer coefficient (h) should be treated as a lumped parameter including the true fluid/solid film heat transfer coefficient (h_{fs}) and the particle conductivity (k_p). The appropriate lumping was shown by Stuke (1948) to be given by

$$\frac{1}{h} = \frac{1}{h_{fs}} + \frac{(d_p/\beta)}{k_p} \tag{29}$$

where $\beta = 10$, 8, and 6 for spheres, cylinders, and slabs, respectively, and d_p is the sphere or cylinder diameter or slab thickness.

The fluid/solid heat transfer coefficient (h_{fs}) is well correlated by Handley and Heggs (1968) in the form

$$Nu_{fs} = \frac{h_{fs}d_p}{k_g} = \frac{0.255}{\epsilon}\,Pr^{1/3}\,Re^{2/3} \tag{30}$$

for $Re > 100$ and $d_t/d_p > 8$. At low values of Re, there is a tremendous scatter (over two orders of magnitude) in estimates of Nu_{fs} obtained by various workers. Estimates of the asymptotic value as $Re \to 0$ vary between about 0.1, which can be inferred from the mass transfer work of Wakao et al. (1976), to 12.4, as measured by Miyauchi et al. (1976). There is obviously a need here for a careful look at the type of experiment best suited to heat or mass transfer studies at low values of Re.

The Fluid/Wall Heat Transfer Coefficient (h_{wf})

The direct determination of h_{wf} from heat transfer experiments is made difficult because of simultaneous heat transfer between the wall and contacting particles. However, it is possible to estimate h_{wf} from mass transfer experiments using a heat and mass transfer analogy. Yagi and Wakao (1959) estimated the wall mass transfer coefficient by measuring the dissolution rate of a coated material on the inner wall of the packed tube to a water stream. By analogy, the fluid/wall heat transfer coefficient is correlated by

$$Nu_{fw} = \frac{h_{wf}\,d_p}{k_g} = \begin{cases} 0.6\,Pr^{1/3}\,Re^{1/2} & (Re\ 1\text{-}40) \\ 0.2\,Pr^{1/3}\,Re^{0.8} & (Re\ 40\text{-}2\,000) \end{cases} \tag{31}$$

Kunii and Suzuki (1968*a*), in a similar experiment, found

$$Nu_{fw} = C\,Pr^{1/3}\,Re^{0.75} \qquad (Re > 100) \tag{32}$$

where

$$C = \frac{0.06}{\epsilon_\omega^2}$$

and ϵ_ω is the average void fraction of the wall region (thickness $= 0.5\,d_p$); ϵ_ω will depend to some extent on the packing and the d_t/d_p ratio. For spheres, Dixon (1978*b*) reports $\epsilon_\omega \simeq 0.5$, with little if any dependency on d_t/d_p.

The validity of the correlation of Yagi and Wakao for low values of Re is in some doubt owing to the neglect of axial dispersion in the analysis of the data.

Olbrich and Potter (1972) measured the vaporization of mercury from the wall into a nitrogen stream. They had to consider also simultaneous axial and radial gas mixing in the voids as well as accounting for the pressure drop across the bed, side effects which were absent in the work of Yagi and Wakao. It is perhaps not surprising that their data, which are correlated by

$$Nu_{fw} = 8.9\,Pr^{1/3}\,Re^{0.34} \qquad (Re\ 100 \sim 3\,000) \tag{33}$$

are substantially different from those of Yagi and Wakao.

The Solid/Wall Heat Transfer Coefficient (h_{ws})

There is little, if any, published data on this parameter.

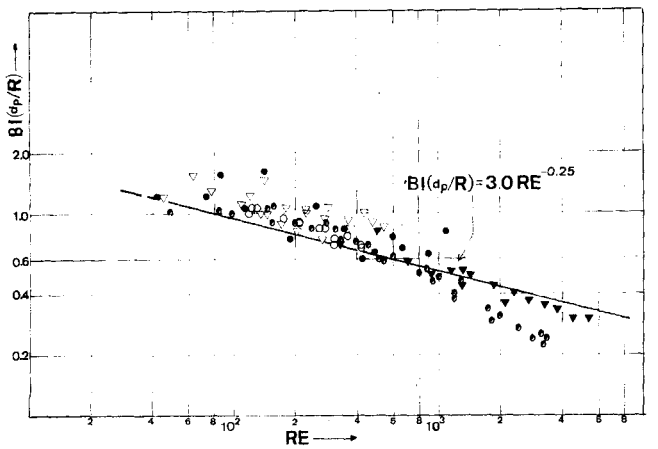

Fig. 2. Comparison of theoretical and experimental Biot numbers. (▽ Dixon et al. (1978), d_t = 70.8 mms, ceramic balls d_p = 6.4, 9.5, 12.7 mms, steel spheres d_p = 9.5 mms; ○ de Wasch and Froment (1972), d_t = 99 mms, V_2O_5 catalyst cylinders, d_p = 5.7 mms; ▼ Kunii et al. (1968), d_t = 140 mms, celite spheres, d_p = 28 mms, 42 mms). ● Coberly and Marshall (1951), d_t = 127 mms, celite cylinders, d_p = 3.6, 7.3, 13.2 mms;* ◓ Calderbank and Pogorsky (1957), d_t = 101.6 mms, alundum spheres d_p = 6.4, 12.7 mms, celite cylinders d_p = 3.6, 7.3 mms.*
*Diameter of equal volume sphere.

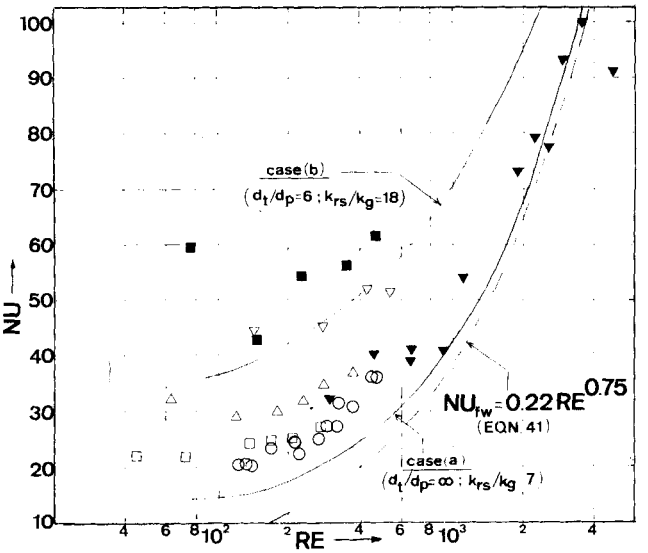

Fig. 3. Comparison of theoretical and experimental Nusselt numbers. (Dixon et al. (1978) ceramic balls, ▽ 12.7 mm, △ 9.5 mm, □ 6.4 mms; steel spheres ■ 9.5 mm; de Wasch and Froment (1972), V_2O_5 cylinders, ○ 5.7 mms; Kunii et al. (1968), celite spheres ▼ 28 mm and 42 mms).

About all we can do at present is estimate a lower bound by considering the ideal case of heat transfer between a plane wall and a contacting hexagonal close packed array of spheres (Olbrich, 1970). For this case

$$h_{ws} = \frac{2.12\, k_{rs}}{d_p} \tag{34}$$

or

$$Bi_s = \frac{h_{ws} R}{k_{rs}} = 2.12\left(\frac{R}{d_p}\right)$$

In practice, when $Bi_s \geq 10$, its effect on the parameter relations in Equations (22) to (24) is unusually small. Thus, unless R/d_p is very small, it should always be permissible to set $Bi_s = \infty$.

DISCUSSION

The Apparent Wall Biot Number (Bi)

The fluid/wall heat transfer coefficient (h_{wf}) can be correlated in terms of a Nusselt number (Nu_{fw}), appearing in Equations (31) to (33), or a Biot number (Bi_f), defined by

$$Bi_f = \frac{h_{wf} R}{k_{rf}} \tag{35}$$

From Equation (35) and the definition of Nu_{fw} in Equation (31), we obtain

$$Bi_f = \left(\frac{R}{d_p}\right) \frac{Nu_{fw} \times Pe_{RF}}{Re \cdot Pr} \tag{36}$$

Nearly all the work on heat transfer in packed beds has used air as the fluid, for which $Pr = 0.72$. Taking $Pe_{RF} = 10$ (for $Re > 40$) and Nu_{fw} from Equation (32), with $\epsilon_\omega = 0.5$, $Bi = Bi_f$ from Equation (22), then the apparent Biot number is given by

$$Bi\left(\frac{d_p}{R}\right) = 3.0\ Re^{-0.25} \tag{37}$$

This important result shows that the apparent wall heat transfer coefficient ($h_{w,\text{eff}}$), if represented in terms of the product $Bi(d_p/R)$, should correlate uniquely with Re for particles of differing sizes and conductivities.

The prediction of Equation (37) is shown in Figure 2 to be fairly close to the experimental data of Dixon et al. (1978*a*), DeWasch and Froment (1972), Kunii et al. (1968*a*), and Calderbank and Pogorsky (1957). Also shown are the estimates of Bi obtained by reanalysis of the data of Coberly and Marshall (1951), using the pseudohomogeneous model, Equations (13) to (20), and employing nonlinear regression analysis. The correlation of Yagi and Wakao for Nu_{fw} [Equation (31)] also gives a prediction of Bi close to experimental values. However, that of Olbrich and Potter [Equation (33)] predicts values of Bi which are much too high.

Nothing definite can be said at present on the Bi vs. Re relationship at low values of Re (say $Re < 40$). Only Yagi and Wakao have measured wall/fluid mass transfer coefficients in this region (from which h_{wf} can be estimated), and their correlation should be treated cautiously since axial dispersion effects were neglected in their analysis. In the analogous problem of fluid/solid heat transfer at low Re, Gunn and DeSouza (1974) report estimates of h_{fs} increased by up to two orders of magnitude when axial conduction effects are included in the model. It will be a difficult matter also to test any theoretical prediction of Bi at low Re, since very short bed depths must be used in practice (typically a few particle diameters). This creates numerous practical difficulties, and, on top of all these, there always remains the nagging problem of deciding on the proper boundary condition to use at the bed exit, a problem which assumes considerable importance for very short beds.

Much of the literature data on the apparent wall heat transfer coefficient is, however, presented in terms of the apparent Nusselt number $Nu = (h_{w,\text{eff}}\, d_p/k_g)$, which is related to the Biot number by

$$Nu = Bi\left(\frac{d_p}{R}\right) \frac{Re\ Pr}{Pe_R} \tag{38}$$

Eliminating Pe_R by Equation (24) and Bi by means of Equations (22) and (36), we obtain

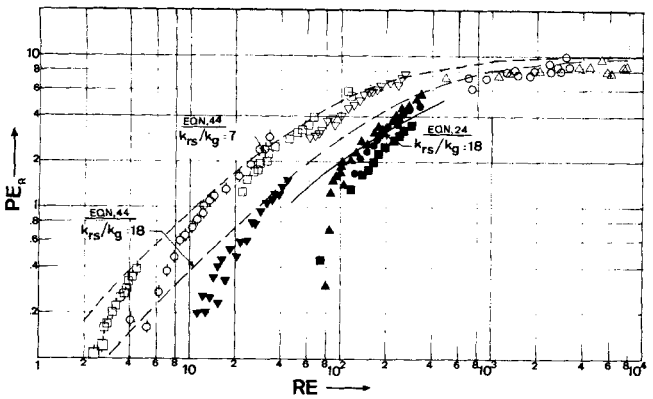

Fig. 4. Radial Peclet number data.

Key to graph:

Symbol	Packing	d_t/d_p	Workers
●	6.8 mm nickel	14.0	Gunn and Khalid (1975)
■	6.4 mm steel	14.9	Gunn and Khalid (1975)
▼	1.0 mm lead	95.2	Gunn and Khalid (1975)
▲	7.0 mm lead	13.6	Gunn and Khalid (1975)
▽	6.0 mm glass	15.9	Gunn and Khalid (1975)
□	0.5 mm glass	190.5	Gunn and Khalid (1975)
○	1.15 mm glass	82.8	Gunn and Khalid (1975)
□	3.0 mm glass	31.8	Gunn and Khalid (1975)
○	28 mm celite	5.0	Kunii et al. (1968)
△	42 mm celite	3.3	Kunii et al. (1968)

$$Nu = 4\beta\,(d_p/R) + Nu_{fw}\left(1 + \beta \cdot \frac{Pe_{RF}}{RePr}\right) \quad (39)$$

where

$$\beta = \frac{(k_{rs}/k_g)}{\left(\frac{8}{N_S} + \frac{Bi_S + 4}{Bi_S}\right)}$$

Unlike the group $Bi(d_p/R)$, the Nusselt number does not correlate uniquely with Re, for a given fluid, but depends, in addition, on the d_t/d_p ratio; the pellet conductivity (k_p), which influences k_{rs}/k_g; the interphase heat transfer coefficient (h_{fs}), through the N_S group; the radial fluid conductivity (k_{rf}); and the solid/wall heat transfer coefficient (h_{ws}). When the data in Figure 2 are replotted in a Nu vs. Re diagram, as in Figure 3, they appear to show a considerable scatter. This spread of the data can be predicted, however, from Equation (39) for limiting cases.

Case (a): $d_t/d_p \to \infty$. In the limit as $d_t/d_p \to \infty$, both N_S and $Bi_s \to \infty$. Equation (39) can be simplified to the form

$$Nu = Nu_{fw}\left\{1 + \frac{10(k_{rs}/k_g)}{Re\ Pr}\right\} \quad (40)$$

if we take $Pe_{RF} = 10$ for $Re > 40$. From Kunii and Suzuki (1968*a*)

$$Nu_{fw} = 0.22\ Re^{0.75} \quad (41)$$

for air ($Pr = 0.72$), assuming $\epsilon_\omega = 0.5$.

For a nonmetallic packing (typically, $k_{rs}/k_g = 7$), Equations (40) and (41) predict the curve given as case (a) in Figure 3.

Case (b): d_t/d_p small. The general Equation (39) must now be used to predict Nu. Case (b) in Figure 3 shows that for metallic packings, the ratio Nu/Nu_{fw} can be as large as 5 at low to moderate Re.

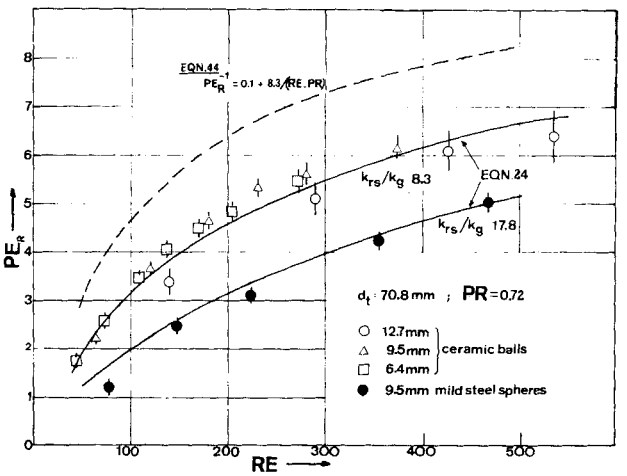

Fig. 5. Comparison of theoretical and experimental radial Peclet numbers.

The Effective Radial Peclet Number (Pe_R)

The vast bulk of the literature data on this parameter concerns heat transfer experiments carried out in large diameter beds of small particles, for which $d_t/d_p \to \infty$. The case of heat transfer in relatively narrow tubes, for which typically $4 \leq (d_t/d_p) \leq 12$, which is one of considerable practical importance, has received insufficient attention.

Most of the literature data have been obtained using models which do not account for axial conduction effects. However, the analysis of Gunn and Khalid (1975) included axial conduction, and the experiments of Kunii et al. (1968*b*) were carried out at very high Re, so that axial conduction effects were negligible. The data of these two groups are shown in Figure 4. Our own data, also accounting for axial conduction, are given in Figure 5, together with their 95% confidence intervals.

The key parameter introducing the effect of a finite d_t/d_p ratio on Pe_R in Equation (24) is the N_S group, which is defined by

$$N_S = \frac{aR^2h}{k_{rs}} \quad (42)$$

Now $R = d_t/2$ and $a = 6(1 - \epsilon)/d_p$ for a spherical packing. Substituting for h from Equation (29) and eliminating h_{fs} in terms of Nu_{fs} from Equation (30), we finally obtain

$$N_S = \frac{1.5\,(1 - \epsilon) \times (d_t/d_p)^2}{\left(\frac{k_{rs}}{k_g}\right)\left\{\frac{1}{Nu_{fs}} + \frac{0.1}{(k_p/k_g)}\right\}} \quad (43)$$

Note first that as $d_t/d_p \to \infty$, $N_S \to \infty$. From Equation (A2) in the Appendix, we have the result

$$t(z, r) \to T(z, r) \quad \text{as} \quad N_S \to \infty$$

In the limit, the two phases attain the same temperature. We also note from the boundary conditions (A4*a*) and (A4*b*) that

$$Bi_s \to Bi_f \quad \text{as} \quad N_S \to \infty$$

Letting $N_S \to \infty$ in Equation (24) leads to the familiar limiting form

$$\frac{1}{Pe_R} = \frac{1}{Pe_{RF}} + \frac{(k_{rs}/k_g)}{Re \cdot Pr} \quad (44)$$

This form of correlation has been used with considerable success by several workers, for example, Kunii et al.

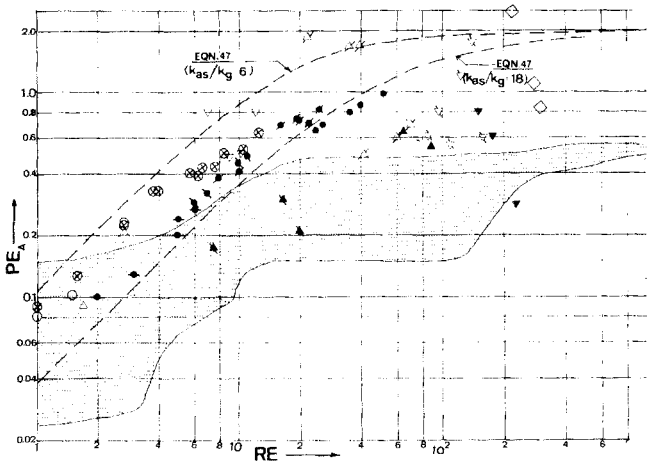

Fig. 6. Axial Peclet number data.

Key to graph

Symbol	Packing	d_t/d_p	Workers
	Various	3.8-12, 19.7, 57.8	Votruba et al. (1972)
⊕	2.6 mm glass	19.2	Yagi et al. (1961)
○	0.9 mm glass	55.6	Yagi et al. (1961)
●	4.8 mm steel	10.4	Yagi et al. (1961)
◪	4.8 mm steel	14.2	Yagi et al. (1961)
◪	3.0 mm steel	22.7	Yagi et al. (1961)
⊷	1.5 mm lead	45.3	Yagi et al. (1961)
△	0.5 mm glass	190.0	Gunn and de Souza (1974)
▽	1.2 mm glass	79.0	Gunn and de Souza (1974)
⧖	2.2 mm glass	43.3	Gunn and de Souza (1974)
⧗	3.0 mm glass	31.8	Gunn and de Souza (1974)
◇	6.0 mm glass	15.9	Gunn and de Souza (1974)
▲	3.2 mm steel	29.8	Gunn and de Souza (1974)
▼	6.3 mm steel	15.1	Gunn and de Souza (1974)
⋈	0.8 mm lead	119.1	Gunn and de Souza (1974)

(1968*b*). Figure 4 shows Equation (44) to predict Pe_R to within 25% for nonmetallic packings such as glass and celite, having an average value of $k_{rs}/k_g = 7$, and using $Pe_{RF}(\infty) = 10$. This is to be expected for the results of Gunn and Khalid, since most of their data involves high d_t/d_p. The data of Kunii et al. were taken at very high Re, so that the first term of Equation (44) dominates and $Pe_R \simeq 10$, which ensures a reasonable fit. Equation (44) is less successful for metallic packings. In these cases, (k_{rs}/k_g) is larger, perhaps 15 to 18, and to maintain a large N_S requires increased d_t/d_p or a very much increased flow rate.

For data such as our own, at low d_t/d_p and moderate Re, we would not expect Equation (44) to be so successful, and this is confirmed in Figure 5. The general Equation (24) should now be used, and the best agreement (to within a few percent) is found for $Bi_S \to \infty$. In the absence of data on the solid/wall heat transfer coefficient (h_{ws}), we recommend that this limiting value of Bi_s be used in computing Pe_R. The data in Figure 5 show that particle diameter has only a weak effect on Pe_R, and the data can be adequately predicted by a single curve for the intermediate d_t/d_p ratio ($= 7.5$) and with $Pe_{RF}(\infty) = 10$.

In Figure 4 we also show the prediction of Equation (24) for the metallic packings of Gunn and Khalid at lower d_t/d_p (13.6 to 14.9) and moderate Re ($50 < Re < 400$). The prediction lies within the data; however, the data appear to have a greater slope, as is the case with virtually all Gunn and Khalid's data. It is not clear why this should be; it is encouraging, however, that Equation (24) predicts the magnitude of the data reasonably well and is a definite improvement over Equation (44).

Finally, we note that as $Re \to 0$, Equation (44) combined with Equation (26) leads to

$$\frac{k^0_{r,\text{eff}}}{k_g} = 0.67\,\epsilon + \frac{k_{rs}}{k_g} \tag{45}$$

the familiar form for stagnant conductivity. The behavior of Equation (24), however, hinges on the behavior of Nu_{fs} and Nu_{fw} as $Re \to 0$. Since this is far from well established in the literature, we can come to no conclusions regarding Equation (24) as $Re \to 0$.

Effective Axial Peclet Number (Pe_A)

Measurements of effective axial thermal conductivity have been made in one of two ways: experiments in adiabatic packed beds, that is, no radial conduction present, or joint estimation with Pe_R and Bi from radial temperature profiles at bed exit. The latter method, used by Dixon et al. (1978*a*) and Gunn and Khalid (1975), tends to give unreliable estimates of Pe_A, as this parameter has little effect on exit profiles. In Figure 6, therefore, we present only results obtained by the first method.

The results show considerable scatter, typically of an order of magnitude, at all Reynolds numbers. There is no clear distinction between metallic and nonmetallic packings; however, the results of Votruba et al. (1972), in all but two cases having $4 \leq d_t/d_p \leq 12$, lie fairly consistently beneath the rest, which were mostly for $d_t/d_p > 20$.

We consider first the experiments made on beds having a large d_t/d_p ratio.

Large (d_t/d_p): In the limit $d_t/d_p \to \infty$, we have from Equation (43) $N_S \to \infty$, and the limiting form of Equation (23) is

$$\frac{1}{Pe_A} = \frac{1}{Pe_{AF}} + \frac{(k_{as}/k_g)}{Re \cdot Pr} \tag{46}$$

Equation (46) shows that when the temperatures of the two phases are equal, $(N_S = \infty)$, the effective axial conductivity, is simply the sum of the conductivities of the two phases. If we use Edwards and Richardson's correlation for Pe_{Am} and substitute into Equation (46), noting $Pe_{AF} = Pe_{Am}$, we obtain

$$\frac{1}{Pe_A} = \frac{0.5}{1 + \epsilon\beta/(RePr)} + \frac{(0.73\,\epsilon + k_{as}/k_g)}{Re \cdot Pr} \tag{47}$$

$$(\beta = 9.7, \text{ air})$$

As a consequence of our choice of correlation for Pe_{AF}, we have the limiting relationships $Pe_A \to 2$ as $Re \to \infty$ and $k^0_{a,\text{eff}}/k_g = 0.73\,\epsilon + k_{as}/k_g$. Had we used the correlations of Hiby (1962) instead, we would have as limits $Pe_A \to 1.54$ as $Re \to \infty$ and $k^0_{a,\text{eff}}/k_g = 0.67\,\epsilon + k_{as}/k_g$.

Taking an average value of $\epsilon = 0.4$ and the limiting cases of $k_{as}/k_g = 6$ (upper dotted curve, nonmetallics) and $k_{as}/k_g = 18$ (lower dotted curve, metallics), we see in Figure 6 that the majority of the data of Yagi et al. (1960) lies within the band so formed. The results of Gunn and DeSouza (1974), on the other hand, display more scatter and tend to lie outside the band. Within the band the data for metallic packings lie on or nearer the lower curve, while those for nonmetallics lie nearer the upper curve, suggesting that particle conductivity produces a secondary ordering of the data.

TABLE 1. COMPARISON OF YAGI AND WAKAO'S METHOD OF DATA ANALYSIS WITH NONLINEAR LEAST SQUARES

Packing	Re	Bed depth, mm	T_w	$(T_{bc})_L$	$(T_b)_L$	$\frac{T_w-(T_b)_L}{T_w-(T_{bc})_L}$	λ_1	Bi (Y/W)	Bi (NLLS)
12.7 mm ceramic balls	536	51	106.6	32.0	42.3	0.862	1.075	0.68	1.60
		178	107.0	53.2	64.0	0.799	1.310	1.12	2.13
		356	105.9	80.5	85.8	0.791	1.340	1.19	2.61
	429	178	106.8	57.0	68.1	0.793	1.333	1.17	2.45
	291	178	106.9	64.0	73.8	0.772	1.408	1.36	2.87
	140	178	106.4	83.5	88.2	0.795	1.326	1.15	4.61
9.5 mm ceramic balls	373	204	103.6	53.5	65.1	0.769	1.417	1.38	2.88
	280	204	103.8	58.5	69.7	0.753	1.469	1.54	3.25
	230	204	104.3	60.5	72.0	0.737	1.520	1.70	3.38
	180	204	104.0	67.0	77.1	0.727	1.552	1.81	3.58
	120	204	104.4	76.0	83.5	0.736	1.525	1.72	3.57

(Small (d_t/d_p): The majority of the data of Votruba et al. (1972) applies to d_t/d_p ratios between 4 and 12. Their broad band of data lies fairly consistently below that of Yagi. In these cases, N_S may not be large, and we have to use the general Equation (23) to predict Pe_A. However, we should note that it is necessary to reduce the asymptotic value of $Pe_{AF}(\infty)$ from the commonly accepted value of 2 to about 0.5 in order to achieve a reasonable prediction of Votruba's data. There is some support for taking this step provided by the mass transfer work of Hsiang and Haynes (1977). Their results in the range $1.4 < (d_t/d_p) < 8$ show considerably enhanced dispersion over that predicted by the correlation of Edwards and Richardson, which takes $Pe_{Am}(\infty) = 2.0$. Unfortunately, their experiments were not conducted at high enough Re to allow the asymptotic value of Pe_{Am} to be determined. Inspection of the axial mass transfer literature reveals an acute shortage of work in the (d_t/d_p) and Re areas of interest here. Hence, the work of Hsiang and Haynes remains uncorroborated.

SELECTION OF DATA

It should be observed in relation to the Bi vs. Re relationship, shown in Figure 2, that a relatively small body of data has been selected from a vast literature on which to examine the theory.

There are a number of factors concerned with the adequacy of the experimental data and the techniques used to analyze the data which require discussion.

First of all, it should be observed from Figure 2 that in the low to moderate range of Re (say $40 \leq Re \leq 400$), the Biot number lies in the range (0.7 to 1.2) $\times$ (R/d_p). Now, the solution of the one-phase model, which is fitted to observed temperature profiles to give estimates of Bi, Pe_R, and Pe_A, becomes insensitive to Bi when $Bi \geq 10$, or when $R/d_p \geq 10$, say. Thus, data collected on beds having large d_t/d_p ratio in this range of Re should be rejected on the grounds that reliable estimates of Bi cannot be obtained from the data.

Our second criticism concerns some of the methods that have been employed to analyze the data. The first group of methods, used by Coberly and Marshall (1951) and later by Plautz and Johnstone (1955), obtains parameter estimates from the original differential equations and boundary conditions, Equations (13) to (20), by substitution of first and second partial derivatives with estimates obtained by numerical differentiation of the data. Even if it were possible to eliminate experimental errors totally, which of course it is not, this approach would still produce biased parameter estimates, owing to the introduction of systematic truncation errors into the approximation of derivatives. In the presence of quite small experimental errors, these estimators also become grossly inefficient.

Perhaps less obvious are the deficiencies in the analysis of Yagi and Wakao (1959), which was followed later by Agnew and Potter (1970). Yagi and Wakao's experimental technique consists of measuring the bed temperature (T_{bc}) along the central axis $(r = 0)$ at several points, the wall temperature (this was assumed to be 100°C and was not actually measured), and the mean exit gas temperature $(T_b)_L$. Taking the first term of the infinite series solution for the plug flow case $(Pe_A = \infty)$, Yagi and Wakao obtained

$$\frac{T_w - T_{bc}}{T_w - T_o} = \frac{2\,Bi \exp\left[-z d_p \lambda_1^2/(R^2 \cdot Pe_R)\right]}{(Bi^2 + \lambda_1^2) \cdot J_0(\lambda_1)} \tag{48}$$

Both Bi and Pe_R were calculated simultaneously from the slope of the straight line portion of the semilogarithmic plot of $T_w - T_{bc}$ vs. z, made according to Equation (48), together with the ratio of the temperature differences at the bed exit

$$\frac{T_w - (T_b)_L}{T_w - (T_{bc})_L} = 2\,\frac{J_1(\lambda_1)}{\lambda_1} \tag{49}$$

and with the help of the equation

$$\lambda_1 J_1(\lambda_1) = Bi\, J_0(\lambda_1) \tag{50}$$

This procedure is appealingly simple but, unfortunately, appears to give estimates of Bi with a large negative bias, as is apparent from a comparison with the results of nonlinear regression on several of our experimental runs, as shown in Table 1.

ACKNOWLEDGMENT

Anthony G. Dixon wishes to acknowledge financial support received from the Science Research Council throughout the period 1975 to 78 and additional support given during leave of absence from the University of Edinburgh in 1977/78 by Professor D. W. T. Rippin, E.T.H. Zürich.

NOTATION

All heat transfer parameters defined in terms of total area (void + nonvoid) normal to the direction of heat transfer.

a = specific interfacial surface area
c_p = fluid specific heat
d_p = pellet diameter
d_t = tube diameter
D_{af} = axial fluid diffusivity
G = superficial mass flow rate

h = apparent fluid/solid heat transfer coefficient
h_{fs} = fluid/solid heat transfer coefficient
$h_{w,eff}$ = apparent wall heat transfer coefficient (one-phase model)
h_{wf} = wall/fluid heat transfer coefficient
h_{ws} = wall/solid heat transfer coefficient
k_{af} = axial conductivity of the fluid
k_{as} = axial conductivity of the solid
$k_{a,eff}$ = axial effective conductivity (one-phase model)
$k^0_{a,eff}$ = stagnant bed axial effective conductivity (one-phase model)
k_{rf} = radial conductivity of the fluid
k_{rs} = radial conductivity of the solid
$k_{r,eff}$ = radial effective conductivity (one-phase model)
$k^0_{r,eff}$ = stagnant bed radial effective conductivity (one-phase model)
k_g = molecular conductivity of the fluid
k_p = pellet conductivity
r = radial coordinate
R = tube radius
t = solid phase temperature
T = fluid phase temperature
T_b = bed temperature (in one-phase model)
T_o = temperature of calming section wall
T_w = temperature of test section wall
u = superficial fluid velocity
z = axial coordinate

Dimensionless Parameters

Bi = apparent Biot number, $h_{w,eff} \cdot R/k_{r,eff}$
Bi_f = fluid/wall Biot number, $h_{wf}R/k_{rf}$
Bi_s = solid/wall Biot number, $h_{ws}R/k_{rs}$
K = ratio of axial to radial solid conductivity, k_{as}/k_{rs}
N_F = interphase heat transfer group, aR^2h/k_{rf}
N_S = interphase heat transfer group, aR^2h/k_{rs}
Nu = apparent wall Nusselt number, $h_{w,eff} \cdot d_p/k_g$
Nu_{fw} = fluid/wall Nusselt number, $h_{wf} \cdot d_p/k_g$
Nu_{fs} = fluid/solid Nusselt number, $h_{fs} \cdot d_p/k_g$
Pe'_A = effective axial Peclet number (based on R), $Gc_pR/k_{a,eff}$
Pe_A = effective axial Peclet number, $Gc_pd_p/k_{a,eff}$
Pe_{AF} = axial fluid Peclet number (based on d_p) Gc_pd_p/k_{af}
Pe'_{AF} = axial fluid Peclet number (based on R) Gc_pR/k_{af}
$\hat{Pe}_{AF}$ = axial Peclet number, defined by Equation (A16)
Pe_{Am} = axial fluid Peclet number (for mass), ud_p/D_{af}
Pe_R = effective radial Peclet number, $Gc_pd_p/k_{r,eff}$
Pe'_R = effective radial Peclet number (based on R) $Gc_pR/k_{r,eff}$
Pe_{RF} = radial fluid Peclet number, Gc_pd_p/k_{rf}
Pe'_{RF} = radial fluid Peclet number (based on R) Gc_pR/k_{rf}
Pr = Prandtl number, $(\mu C_p/k_g)$
Re = Reynolds number, Gd_p/μ
t^* = dimensionless solid temperature, $(t - T_o)/(T_w - T_o)$
T^* = dimensionless fluid temperature, $(T - T_o)/(T_w - T_o)$
x = normalized axial coordinate, z/R
y = normalized radial coordinate, r/R

Greek Letters

α = defined in Equation (A11)
β = defined by Equation (A19)
$\hat{\beta}$ = defined by Equation (A34)
β' = defined by Equation (A27)
γ' = defined by Equation (A17)
ϵ = mean bed voidage
ϵ_ω = mean voidage of wall region (thickness = $d_p/2$)
θ = dimensionless bed temperature, $(T_b - T_o)/(T_w - T_o)$
μ = fluid viscosity

LITERATURE CITED

Agnew, J. B., and O. E. Potter, "Heat Transfer Properties of Packed Tubes of Small Diameter," *Trans. Inst. Chem. Engrs.*, 48, T15 (1970).

Bischoff, K. B., "A Note on Gas Dispersion in Packed Beds," *Chem. Eng. Sci.*, 24, 607 (1969).

Calderbank, P. H., and L. A. Pogorsky, "Heat Transfer in Packed Beds," *Trans. Inst. Chem. Engrs.*, 35, 195 (1957).

Coberly, C. A., and W. R. Marshall, "Temperature Gradients in Gas Streams Flowing Through Fixed Granular Beds," *Chem. Eng. Progr.*, 47, 141 (1951).

De Wasch, A. P., and G. F. Froment, "Heat Transfer in Packed Beds," *Chem. Eng. Sci.*, 27, 567 (1972).

Dixon, A. G., D. L. Cresswell, and W. R. Paterson, "Heat Transfer in Packed Beds of Low Tube/Particle Diameter Ratio," *ACS Symposium Ser. No. 65*, 238 (1978*a*).

Dixon, A. G., "Heat Transfer in Packed Beds of Low Tube/Particle Diameter Ratio," Ph.D. thesis, Univ. Edinburgh, Scotland (1978*b*).

Edwards, M. F., and J. F. Richardson, "Gas Dispersion in Packed Beds," *Chem. Eng. Sci.*, 23, 109 (1968).

Fahien, R. A., and J. M. Smith, "Mass Transfer in Packed Beds," *AIChE J.*, 1, 28 (1955).

Gunn, D. J., and M. Khalid, "Thermal Dispersion and Wall Heat Transfer in Packed Beds," *Chem. Eng. Sci.*, 30, 261 (1975).

Gunn, D. J., and D. Pryce, "Dispersion in Packed Beds," *Trans. Inst. Chem. Engrs.*, 47, T341 (1969).

Gunn, D. J., and J. F. C. De Souza, "Heat Transfer and Axial Dispersion in Packed Beds," *Chem. Eng. Sci.*, 29, 1363 (1974).

Handley, D., and P. J. Heggs, "Momentum and Heat Transfer Mechanisms in Regular Shaped Packings," *Trans. Inst. Chem. Engrs.*, 46, T251 (1968).

Hiby, J. W., "Longitudinal and Transverse Mixing During Single Phase Flow Through Granular Beds," in *Interaction Between Fluids and Particles*, P. A. Rottenburg, p. 312, Institute of Chemical Engineers, London, England (1962).

Hsiang, T., Chu-Shao, and H. W. Haynes, Jr., "Axial Dispersion in Small Diameter Beds of Large Spherical Particles," *Chem. Eng. Sci.*, 32, 687 (1977).

Kunii, D., and M. Suzuki, Paper presented to Symposium on Heat and Mass Transfer, Minsk (1968*a*).

———, and N. Ono, "Heat Transfer from Wall Surface to Packed Beds at High Reynolds Number," *J. Chem. Eng. (Japan)*, 1, 21 (1968*b*).

Kunii, D., and J. M. Smith, "Heat Transfer Characteristics of Porous Rocks: II. Thermal Conductivities of Unconsolidated Particles with Flowing Fluids," *AIChE J.*, 7, 29 (1961).

Littmann, H., and D. E. Sliva, "Gas-Particle Heat Transfer Coefficients in Packed Beds at Low Reynolds Numbers," Fourth International Heat Transfer Conference, Paris-Versailles, 1, CT 1.4 (1970).

Miyauchi, H., H. Kataoka, and T. Kikuchi, "Gas Film Coefficients of Mass Transfer in Low Peclet Number Region for Sphere Packed Beds," *Chem. Eng. Sci.*, 31, 9 (1976).

Olbrich, W. E., "A Two-Phase Diffusional Model to Describe Heat Transfer Processes in a Non-Adiabatic Packed Tubular Bed," *Chemeca '70*, Proceedings of a Conference, Melbourne and Sydney, Aug. 19-26 (1970), p. 101, Butterworth, London, England (1971).

———, and O. E. Potter, "Mass Transfer from the Wall in Small Diameter Packed Beds," *Chem. Eng. Sci.*, 27, 1733 (1972).

Plautz, D. A., and H. F. Johnstone, "Heat and Mass Transfer in Packed Beds," *AIChE J.*, 1, 193 (1955).

Roemer, G., J. S. Dranoff, and J. M. Smith, "Diffused in Packed Beds at Low Flow Rates," *Ind. Eng. Chem. Fundamentals*, 1, 284 (1962).

Stuke, B., "Berechnung des Wärmeaustausches in Regeneratoren mit zylindrischen und kugelförmigen Füllmaterial," *Angewandte Chemie*, B20, 262 (1948).

Villadsen, J., and M. Michelsen, *Solution of Differential Equation Models by Polynomial Approximation*, Prentice-Hall, Englewood Cliffs, N.J. (1978).
Vortmeyer, D., and R. J. Schaefer, "Equivalence of One- and Two-Phase Models for Heat Transfer Processes in Packed Beds: One-Dimensional Theory," *Chem. Eng. Sci.*, **29**, 485 (1974).
Votruba, J., V. Hlavacek, and M. Marek, "Packed Bed Axial Thermal Conductivity," *ibid.*, **27**, 1845 (1972).
Wakao, N., K. Tanaka, and H. Nagai, "Measurement of Particle-To-Gas Mass Transfer Coefficients from Chromatographic Adsorption Experiments," *ibid.*, **31**, 1109 (1976).
Willhite, G. P., D. Kunii, and J. M. Smith, "Heat Transfer in Beds of Fine Particles (Heat Transfer Perpendicular to Flow)," *AIChE J.*, **8**, 340 (1962).
Yagi, S., and H. Wakao, "Heat and Mass Transfer from Wall to Fluid in Packed Beds," *ibid.*, **5**, 79 (1959).
———, and D. Kunii, "Studies on Axial Effective Thermal Conductivities in Packed Beds," *ibid.*, **6**, 543 (1960).
Zehner, P., and E. P. Schlünder, "Wärmeleitfähigkeit von Schüttungen bei mässigen Temperaturen," *Chemie-Ingenieur Technik*, **42**, 933 (1970).

APPENDIX

Two-Phase Model

The two-phase model equations are, in dimensionless form

$$\frac{\partial T^*}{\partial x} = \frac{1}{Pe'_{RF}}\left(\frac{\partial^2 T^*}{\partial y^2} + \frac{1}{y}\frac{\partial T^*}{\partial y}\right) + \frac{1}{Pe'_{AF}}\frac{\partial^2 T^*}{\partial x^2} - \frac{N_F(T^* - t^*)}{Pe'_{RF}} \tag{A1}$$

$$\left(\frac{\partial^2 t^*}{\partial y^2} + \frac{1}{y}\frac{\partial t^*}{\partial y}\right) + K\frac{\partial^2 t^*}{\partial x^2} + N_S(T^* - t^*) = 0 \tag{A2}$$

with boundary conditions

$$y = 0: \quad \frac{\partial T^*}{\partial y} = \frac{\partial t^*}{\partial y} = 0 \tag{A3}$$

$$y = 1: \quad \frac{\partial T^*}{\partial y} + Bi_f T^* = \begin{cases} 0 & x < 0 \\ Bi_f & x > 0 \end{cases} \tag{A4a}$$

$$\frac{\partial t^*}{\partial y} + Bi_s t^* = \begin{cases} 0 & x < 0 \\ Bi_s & x > 0 \end{cases} \tag{A4b}$$

$$T^*, t^* \to 1 \quad \text{as} \quad x \to \infty$$
$$T^*, t^* \to 0 \quad \text{as} \quad x \to -\infty \tag{A5}$$

$$x = 0: \quad T^*(0^+) = T^*(0^-); \quad t^*(0^+) = t^*(0^-) \tag{A6}$$

$$\frac{\partial T^*(0^+)}{\partial x} = \frac{\partial T^*(0^-)}{\partial x}; \quad \frac{\partial t^*(0^+)}{\partial x} = \frac{\partial t^*(0^-)}{\partial x} \tag{A7}$$

We first discretize the radial derivatives in this system by a one-point collocation technique, as described by Villadsen and Michelson (1978). We choose as our collocation point the zero of $P_1^{(0,0)}(y^2)$, a choice guided by consideration of the boundary conditions (A4*a*) and (A4*b*). Denote this by $y_1 (= 1/\sqrt{2})$ and further let $y_2 = 1$. Then we write $T^*(x, y_i) = T_i^*(x)$ and, similarly, $t^*(x, y_i) = t_i^*(x)$. Then, suppressing arguments, we write

$$\left(\frac{\partial^2 T^*}{\partial y^2} + \frac{1}{y}\frac{\partial T^*}{\partial y}\right)_{y=y_1} = -8\,T_1^* + 8\,T_2^* \tag{A8}$$

$$\left(\frac{\partial T^*}{\partial y}\right)_{y=1} = -4\,T_1^* + 4\,T_2^* \tag{A9}$$

Substituting (A8) into (A1) and eliminating T_2^* via the wall boundary condition (A4*a*) and (A9), we have

$$\frac{1}{Pe'_{AF}}\frac{d^2 T_1^*}{dx^2} - \frac{dT_1^*}{dx} - \left(\gamma + \frac{N_F}{Pe'_{RF}}\right)T_1^* + \frac{N_F}{Pe'_{RF}}t_1^* = \begin{cases} -\gamma (x > 0) \\ 0 (x < 0) \end{cases} \tag{A10}$$

where

$$\gamma = \frac{8\,Bi_f}{Pe'_{RF}\,(Bi_f + 4)}$$

Similarly, Equation (A2) becomes

$$\epsilon \cdot \frac{d^2 t_1^*}{dx^2} - \left(\alpha + \frac{N_S}{8}\right)t_1^* + \frac{N_S}{8}T_1^* = \begin{cases} -\alpha (x > 0) \\ 0 (x < 0) \end{cases} \tag{A11}$$

where $\epsilon = K/8$ and $\alpha = Bi_S/(Bi_S + 4)$.

The solution of this coupled pair of boundary value problems requires the roots of the fourth degree characteristic polynomial. These must be found numerically, owing to the complexity of the parameters. An exact solution to (A10) and (A11) is possible under certain restrictive assumptions: $T_1^* = t_1^*$ or $K = 0$. We prefer to develop an approximate solution via perturbation methods.

As is shown by our notation above, we use $\epsilon = K/8$ as perturbation parameter, which will be approximately 0.125. Hence, we are perturbing away from the solution obtained under the second assumption above.

Let

$$t_1^*(x, \epsilon) = \sum_{m=0}^{\infty} \epsilon^m \psi_m(x) \tag{A12}$$

Substituting (A12) into (A11) and equating coefficients of like powers of ϵ, we get

$$\psi_0 = \begin{cases} \left(\frac{N_S}{8}\cdot T_1^* + \alpha\right) \Big/ \left(\frac{N_S}{8} + \alpha\right) & x > 0 \\ \frac{N_S}{8}T_1^* \Big/ \left(\frac{N_S}{8} + \alpha\right) & x < 0 \end{cases} \tag{A13}$$

and

$$\psi_m = \psi''_{m-1} \Big/ \left(\frac{N_S}{8} + \alpha\right) \qquad m \geq 1$$
$$= \left(\frac{N_S}{8}\right) T_1^{*(2m)} \Big/ \left(\frac{N_S}{8} + \alpha\right)^{m+1} \tag{A14}$$

If we truncate (A12) after $k + 1$ terms and substitute into (A10), we are left with an order $2k$ ODE in T_1^*. Hence, it is practical to consider only $k = 1$, giving

$$\frac{1}{P\hat{e}_{AF}}\frac{d^2 T_1^*}{dx^2} - \frac{dT_1^*}{dx} - \gamma' T_1^* = \begin{cases} \gamma' (x > 0) \\ 0 (x < 0) \end{cases} \tag{A15}$$

where

$$\frac{1}{P\hat{e}_{AF}} = \frac{1}{Pe'_{AF}} + \frac{\epsilon N_S N_F}{8\,Pe'_{RF}\left(\frac{N_S}{8} + \alpha\right)^2} \tag{A16}$$

and

$$\gamma' = \gamma + \frac{\alpha N_F}{Pe'_{RF}\left(\frac{N_S}{8} + \alpha\right)} \tag{A17}$$

The solution of Equation (A15) is straightforward; the constants of integration are obtained via the boundary conditions at $x = \pm\infty$ and the continuity conditions at $x = 0$:

$$T_1^*(x) = \begin{cases} 1 - \frac{(1+\beta)}{2\beta}\exp\left\{\frac{P\hat{e}_{AF}x\,(1-\beta)}{2}\right\} & x > 0 \\ \frac{(\beta - 1)}{2\beta}\exp\left\{\frac{P\hat{e}_{AF}x(1+\beta)}{2}\right\} & x < 0 \end{cases} \tag{A18}$$

where

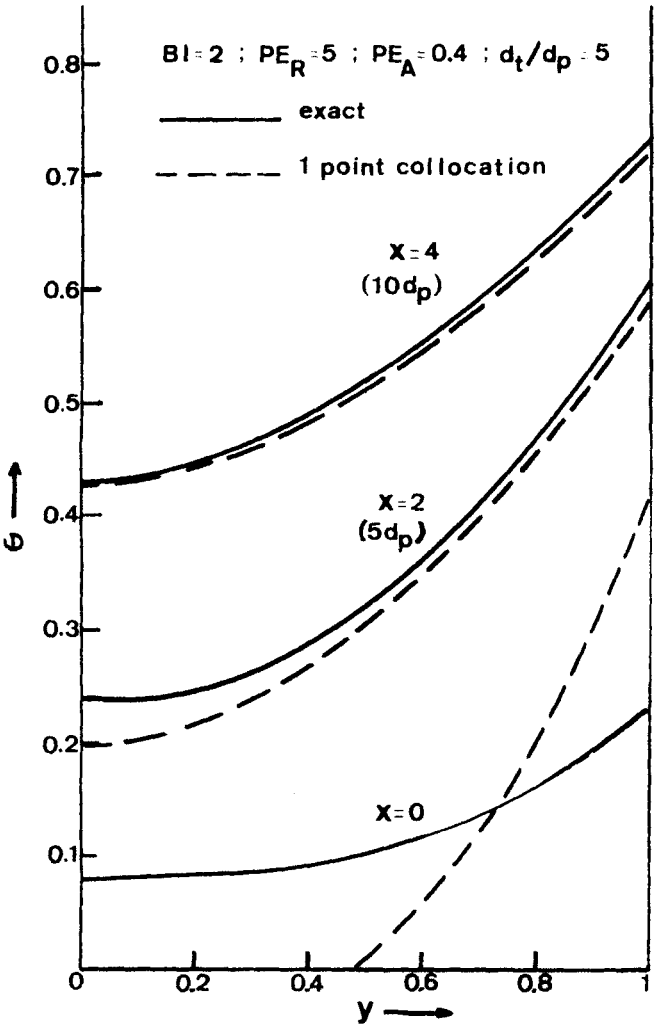

Fig. A1. Comparison of one-point collocation and exact solution of one-phase model.

$$\beta = \sqrt{1 + \frac{4}{P\hat{e}_{AF}}\gamma'} \tag{A19}$$

The final approximate solution is found by interpolation between T_1^* and T_2^*:

$$T^*(x,y) = \begin{cases} 1 + \dfrac{\{Bi_f(y^2-1)-2\}}{Bi_f+4}\left(\dfrac{1+\beta}{\beta}\right)\exp\left\{\dfrac{P\hat{e}_{AF}x(1-\beta)}{2}\right\} & (x>0) \\ \dfrac{\{Bi_f(y^2-1)-2\}}{Bi_f+4}\left(\dfrac{1-\beta}{\beta}\right)\exp\left\{\dfrac{P\hat{e}_{AF}x(1+\beta)}{2}\right\} & (x<0) \end{cases} \tag{A20}$$

One-Phase Model

The dimensionless form of the one-phase model is

$$\frac{1}{Pe'_R}\left(\frac{\partial^2\theta}{\partial y^2}+\frac{1}{y}\frac{\partial\theta}{\partial y}\right)+\frac{1}{Pe'_A}\frac{\partial^2\theta}{\partial x^2}=\frac{\partial\theta}{\partial x} \tag{A21}$$

$$\frac{\partial\theta}{\partial y}=0 \quad \text{at} \quad y=0 \tag{A22}$$

$$\frac{\partial\theta}{\partial y}+Bi\theta=\begin{cases} Bi & (x>0) \\ 0 & (x<0) \end{cases} \quad \text{at} \quad y=1 \tag{A23}$$

$$\theta\to 1 \quad \text{as} \quad x\to\infty; \quad \theta\to 0 \quad \text{as} \quad x\to-\infty \tag{A24}$$

$$\theta(0^+)=\theta(0^-); \quad \frac{\partial\theta(0^+)}{\partial x}=\frac{\partial\theta(0^-)}{\partial x} \tag{A25}$$

The radial derivatives are again discretized by collocation, resulting in a single-boundary value problem. This is solvable analytically and the procedure is routine, so we merely give the result here:

$$\theta(x,y) = \begin{cases} 1+\left\{\dfrac{Bi(y^2-1)-2}{Bi+4}\right\}\left(\dfrac{1+\beta'}{\beta'}\right)\exp\left\{\dfrac{Pe'_Ax(1-\beta')}{2}\right\} & x>0 \\ \left\{\dfrac{Bi(y^2-1)-2}{Bi+4}\right\}\left(\dfrac{1-\beta'}{\beta'}\right)\exp\left\{\dfrac{Pe'_Ax(1+\beta')}{2}\right\} & x<0 \end{cases} \tag{A26}$$

where

$$\beta' = \sqrt{1+\frac{32\,Bi/(Bi+4)}{Pe'_APe'_R}} \tag{A27}$$

Relations between Parameters

By inspection of Equations (A20) and (A26), the two solutions are identical at all points (x, y) if

$$Bi = Bi_f \tag{A28}$$

$$Pe'_A = \hat{Pe}_{AF} \tag{A29}$$

$$\beta = \beta' \tag{A30}$$

Equation (A29) can be written in the form

$$\frac{1}{Pe'_A}=\frac{1}{Pe'_{AF}}+\frac{\epsilon N_S N_F}{8\,Pe'_{RF}\left(\dfrac{N_S}{8}+\alpha\right)^2} \tag{A31}$$

Multiplying throughout by R/dp and noting that

$$\frac{\epsilon N_F N_S}{Pe_{RF}}=\frac{1}{8}\frac{(k_{as}/k_g)N_S^2}{RePr}$$

we obtain the result

$$\frac{1}{Pe_A}=\frac{1}{Pe_{AF}}+\frac{(k_{as}/k_g)}{Re\cdot Pr}\frac{1}{\left(1+\dfrac{8\alpha}{N_S}\right)^2} \tag{A32}$$

From Equations (A30) and (A29)

$$\frac{1}{Pe'_R}=\frac{1}{Pe'_{RF}}\left\{1+\frac{(N_F/8)\alpha}{\left(\dfrac{N_S}{8}+\alpha\right)\hat{\beta}}\right\} \tag{A33}$$

where

$$\hat{\beta} = Bi/(Bi+4) \tag{A34}$$

Multiplying throughout by R/d_p and noting that

$$\frac{N_F}{Pe_{RF}}=\frac{(k_{rs}/k_g)N_S}{Re\cdot Pr}$$

we obtain

$$\frac{1}{Pe_R}=\frac{1}{Pe_{RF}}+\frac{(k_{rs}/k_g)}{Re\cdot Pr}\frac{1}{\hat{\beta}}\frac{1}{\left(\dfrac{1}{\alpha}+\dfrac{8}{N_S}\right)} \tag{A35}$$

Accuracy of Approximate Solutions

The validity of the parameter relations given by Equations (A28), (A32), and (A35) must ultimately stand or fall by

their agreement with reliable experimental data. However, we shall feel more confident if the semianalytical solutions found above provide good approximations to the exact solutions. This question is best examined in two stages: Accuracy of one-point collocation approximation to radial profiles and accuracy of perturbation approximation to axial profiles.

Collocation Approximation

We consider the one-phase model and compare in Figure A1 the one-point collocation solution with the exact analytical solution for a typical case found in our experiments. The axial distances taken correspond to the bed entrance and depths of 5 d_p and 10 d_p. It is apparent that the approximate solution is poor at bed entrance but improves rapidly with increasing bed depth, being within 2% of the exact solution at a depth of 10 d_p.

Villadsen and Michelsen (1978) have proposed a one-point optimal collocation method based on choosing the collocation point as a function of Bi to cover the change in type of the wall boundary condition with varying Bi. In our case, we would take

$$y_1 = \sqrt{\frac{1}{3}\left(\frac{Bi+6}{Bi+4}\right)}$$

However, this choice of collocation point leads to much more complicated parameter relationships for Pe_A and Pe_R. Numerically, these give very similar results to our previous relationships, and we do not consider the refinement to be worth the extra complication.

Perturbation Approximation

Analysis of truncation error in the perturbation expansion is extremely difficult. However, for specific values of the parameters, we may solve the coupled boundary value Equations (A10) and (A11) as accurately as desired by finding the roots of the characteristic polynomial. This solution may then be compared with that given by the perturbation technique.

By examining the truncated series for t_1^* we anticipate worst case conditions regarding accuracy when N_S is small. We see that N_S is small for small (d_t/d_p), large (k_{rs}/k_g), and small Nu_{fs}, that is, small Re. We therefore take $(k_{rs}/k_g) = 18$, $(d_t/d_p) = 7.5$ and investigate the effect of Re on the accuracy of the perturbation solution.

Equations (A10) and (A11) may be reduced to the fourth-order equation

$$\frac{K}{Pe'_{AF}}\cdot\frac{d^4T_1^*}{dx^4} - K\frac{d^3T_1^*}{dx^3} - \left\{\frac{(N_S+8)}{Pe'_{AF}} + \frac{K}{Pe'_{RF}}\cdot[N_F + 8\,Bi_f/(Bi_f+4)]\right\}\frac{d^2T_1^*}{dx^2} + (N_S+8)\frac{dT_1^*}{dx} + \frac{8}{Pe'_{RF}}\left\{\frac{(N_S+8)Bi_f}{Bi_f+4} + N_F\right\}T_1^* = \begin{cases}\dfrac{8}{Pe'_{RF}}\left\{\dfrac{(N_S+8)Bi_f}{Bi_f+4} + N_F\right\} & (x>0)\\ 0 & (x<0)\end{cases} \tag{A36}$$

where we have taken $Bi_s = \infty$.

Case (1) Re = 50. We obtain $Pe'_{RF} = 34.9$, $Pe'_{AF} = 8.18$, $Bi_f = 3.97$, $K = 1$, and, extending the Handley-Heggs correlation slightly, $N_S = 21.94$, $N_F = 102.1$.

The characteristic equation is

$$0.12\,D^4 - D^3 - 6.70\,D^2 + 29.94\,D + 26.82 = 0$$

The roots are found graphically, and after some algebra the solution is

$$T_1^* = \begin{cases} 1 + 0.033\,e^{-6.2x} - 0.894\,e^{-0.8x} & x>0\\ 0.148\,e^{4.1x} - 0.0085\,e^{11.1x} & x<0\end{cases}$$

$$t_1^* = \begin{cases} 1 - 0.088\,e^{-6.2x} - 0.662\,e^{-0.8x} & x>0\\ 0.259\,e^{4.1x} + 0.002\,e^{11.1x} & x<0\end{cases}$$

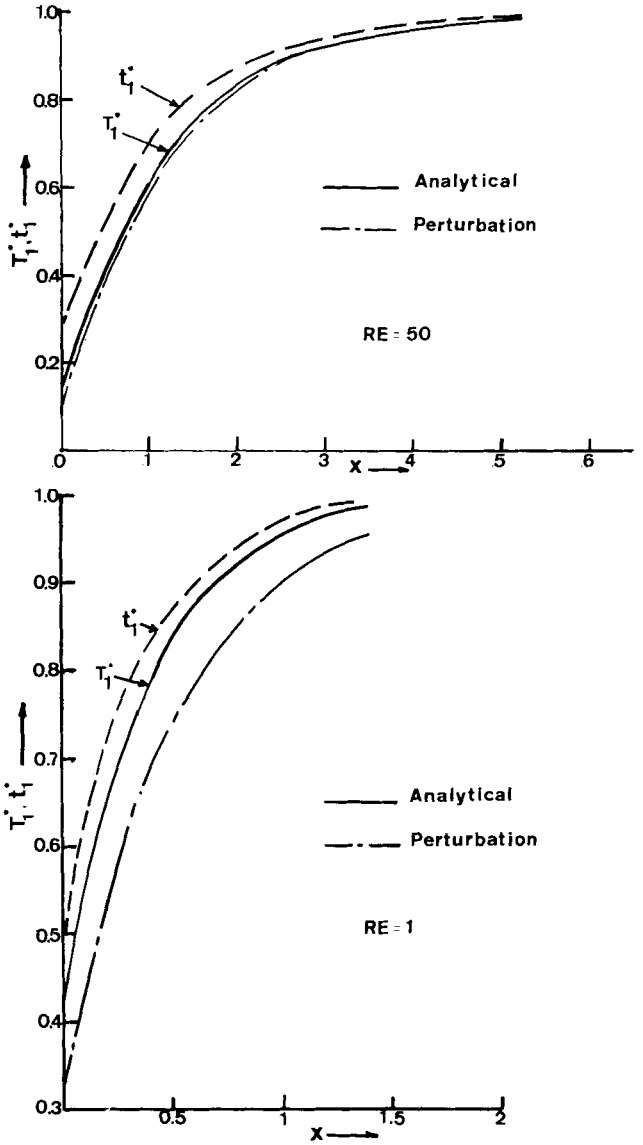

Fig. A2. Comparison of perturbation and analytical solutions of the collocated two-phase model equations.

The perturbation solution gives for T_1^* and $x > 0$

$$T_1^* = 1 - 0.88\,e^{-0.77x}$$

Comparison of the two expressions for T_1^* shows extremely good agreement, illustrated graphically in Figure A2.

As an aside, we may further note that the solid and fluid phase temperatures given here from the exact solution are significantly different.

Case (2) Re = 1. This is the lowest Re value for which we use our predictions. For this case, the characteristic equation is

$$0.13\,D^4 - D^3 - 16.31\,D^2 + 10.16\,D + 121.23 = 0$$

The solutions are given as

$$T_1^* = \begin{cases} 1 + 0.062\,e^{-7.7x} - 0.64\,e^{-2.7x} & x>0\\ 0.416\,e^{2.9x} + 0.0036\,e^{15.6x} & x<0\end{cases}$$

$$t_1^* = \begin{cases} 1 - 0.002\,e^{-7.7x} - 0.505\,e^{-2.7x} & x>0\\ 0.487\,e^{2.9x} + 0.0003\,e^{15.6x} & x<0\end{cases}$$

The perturbation solution is

$$T_1^* = 1 - 0.69\,e^{-1.95x} \quad x<0$$

The comparison is again shown in Figure A2. Agreement is not so good in this case, as expected. However, we should reiterate that this is a worst case example which perhaps suffers further in accuracy from the choice of a correlation for h_{fs} which predicts $Nu_{fs} \to 0$ as $Re \to 0$. In the vast majority of cases, having substantially lower k_{rs}/k_g, higher Re, and perhaps larger d_t/d_p, the accuracy will be as good if not better than that shown in the upper diagram of Figure A2.

Manuscript received July 12, 1978; revision received March 1, and accepted March 23, 1979.

Hot Wire Measurement in the Interacting Two-Plane Parallel Jets

SHINICHI YUU
FUMIO SHIMODA
and
TOMOSADA JOTAKI

Kyushu Institute of Technology
Tobata, Kitakyushu 804, Japan

This study presents the data of turbulence properties in the two-plane parallel air jets which merge as they issue into still surroundings. These turbulent properties (time averaged and root mean square velocities, Eulerian auto and cross correlation coefficients, various scales of turbulence, energy spectra, and probability density functions of fluctuating velocities) were measured in both the converging and combined regions of the jets by using the X array, hot wire anemometers.

The negative high shear stress existed in the merging region. Strictly speaking, the turbulent flow in this region is not isotropic. In the combined region, the turbulent mechanics of these jets are essentially the same as that of the single plane jet. All of the spectra in these jets had a slope of 5/3 over about one decade of the wave number space. The probability density functions were Gaussian except for the boundary to the surrounding air.

SCOPE

Two parallel jets interact with each other and tend to merge into a single jet at the downstream of the jets when they issue from adjacent two nozzles into still surroundings. The interacting turbulent jets are able to accomplish rapid and complete mixing of fluids. These flows have numerous important applications, for example, thrust augmentors, waste disposal plumes from stacks and combustion systems, and significant problems of turbulent diffusion. The mechanism of these apparatus and systems is dominated by the turbulence phenomena of the flow in the jets.

Miller and Comings (1960) and Marsters (1977) have studied the mean flow quantities and the intensities of the turbulent velocity in interacting two plane jets. Becker and Booth (1975) have reported the data of the mean smoke concentration and the intensities of the turbulent concentration in two round jets with nozzle axes intersecting. However, no information about other important turbulent properties in the interacting jet flow is available in the literature.

The main difficulty confronted in application of turbulent theories to various engineering operations comes from insufficient information about the turbulent structure. Hence, in this study, detailed various turbulence properties (time averaged and root mean square velocities, Eulerian auto and cross correlation coefficients, various scales of turbulence, energy spectra, and probability density functions of fluctuating verocities) wire measured in the interacting two plane parallel jets.

Turbulence properties were measured in order to supply engineering information and to give experimental data on which a realistic model of the turbulent flow can be based.

The objective of this work is to describe the flow of air in interacting plane jets with particular emphasis on the structure of turbulence in order to contribute basic data to various engineering operations.